

# Suitability of depleted gas reservoirs for geological CO<sub>2</sub> storage: A simulation study

Arshad Raza<sup>1</sup>, Raoof Gholami<sup>1</sup>, Reza Rezaee<sup>2</sup>, Amanat Ali Bhatti<sup>3</sup>, Chua Han Bing<sup>4</sup>, Vamegh Rasouli<sup>5</sup>

1-Department of Petroleum Engineering, Curtin University, Malaysia

E-Mail: Arshadraza212@gmail.com

2-Department of Petroleum Engineering, Curtin University, Australia

3-Department of Petroleum and Gas Engineering, UET Lahore, Pakistan

4-Department of Chemical Engineering, Curtin University, Malaysia

5- Department of Petroleum Engineering, University of North Dakota, USA

## Abstract

Hydrocarbon reservoirs, particularly depleted gas formations, are promising geological sites for carbon dioxide (CO<sub>2</sub>) storage. Although there have been many studies on the storage aspects of gas reservoirs, suitability of these formations in terms of fluid types such as dry, wet, condensate have not been properly addressed at the reservoir level. In this study, an attempt was made to evaluate different gas reservoirs in order to provide an insight into their storage capabilities. A dynamic numerical simulation was done to simulate CO<sub>2</sub> injection in a synthetic but realistic model of a geologic formation having dry, wet or condensate gas. The obtained results at particular conditions revealed that the condensate gas medium offers a good storage potential, favorable injectivity and reasonable pressure buildup over a long period of time, whilst dry gas formations were found to be the least favorable sites for storage among gas reservoirs. A sensitivity analysis was done to evaluate the injection rate and permeability variation of different media during and after storage. It was indicated that the storage behavior of gas reservoirs is sensitive to the injection rate and selection of an optimum injection rate may help to achieve a good storage capacity in condensate gas systems. The results also highlighted that CO<sub>2</sub> immobilization in gas reservoirs after injection is enhanced due to the reduction of permeability, while no heterogeneity effect was observed under different permeability realizations.

**Keywords:** CO<sub>2</sub> storage, depleted gas reservoirs, numerical simulation, trapping mechanisms

## 1. Introduction

Capturing of Carbon dioxide (CO<sub>2</sub>) from the combustion of fossil fuels and injection it into subsurface geologic formations for permanent storage has been widely recognized as one of the reliable strategy to reduce the amount of CO<sub>2</sub> emission into the atmosphere. Deep saline aquifers, depleted oil and gas reservoirs, and coal-bed seams are possible sites for CO<sub>2</sub> storage.<sup>1</sup> However, depleted oil and gas reservoirs are often the best options as they already hosted hydrocarbon for thousands of years. These petroleum fluids systems are generally divided into five categories of black oil, volatile oil, condensate gas, wet gas, and dry gas. Out of these categories, gas reservoirs which are classified into dry, wet and condensate gas bearing formations<sup>2, 3</sup> have gained the attention of many researchers in recent years as a better place to store CO<sub>2</sub> compared to oil reservoirs due to the high compressibility of gas.<sup>4, 5</sup>

For instance, Gorgon Carbon Dioxide Injection project in Australia has been initiated and is in its construction phase for deployment of CO<sub>2</sub> in a gas field.<sup>6</sup>

There have been many studies carried out to show the potential of injecting CO<sub>2</sub> into dry gas<sup>7-15</sup> and condensate gas reservoirs<sup>4, 16-19</sup> using numerical modeling techniques. According to these studies, the success of a CO<sub>2</sub> storage practice is linked to the injection strategy, reservoir characteristics and operational parameters. For instance, Oldenburg *et al.*<sup>15</sup> studied the storage by focusing on physical processes associated with injections through a numerical simulation. The results obtained indicated that injection allows additional production of methane during or after injection. Jikich *et al.*<sup>9</sup> numerically considered the effects of the injection strategy and operational parameters on CO<sub>2</sub> storage. They concluded that injection after field abandonment can provide a better recovery compared to injection at early stages. In a similar study, Al-Hashami *et al.*<sup>7</sup> showed that CO<sub>2</sub> solubility in brine is favorable to delay the breakthrough time and CO<sub>2</sub> injection at later stages will be more effective in terms of methane production. Polak and Grimstad<sup>12</sup> developed a numerical approach to evaluate CO<sub>2</sub> storage in the Atzbach-Schwanenstadt gas field of Austria. They found a quick breakthrough of CO<sub>2</sub> which could ultimately limit production. They also reported that the reservoir pressure stabilizes after the stoppage of injection and only 10% of injected CO<sub>2</sub> dissolves in the immobile reservoir water during 1500 years with leakage from other wells. Feather and Archer<sup>8</sup> numerically analyzed the factors favorable to enhance natural gas recovery by carbon dioxide injection for storage purposes. They considered well types, permeability, reservoir geometry, injection timing, and injection rate in their modeling. They found that vertical wells, reservoir geometry and low permeable isotropic homogeneous reservoirs are favorable for a successful storage job. Pamukcu *et al.*<sup>14</sup> focused on numerical modeling to predict the short term (less than a decade) system performance of CO<sub>2</sub> injection in the In-Salah gas field. They indicated that CO<sub>2</sub> can reach the northern part of the gas field in 2010 and spread out over an area including production wells in 2015. Khan *et al.*<sup>10</sup> illustrated the potential of CO<sub>2</sub> storage in natural gas reservoirs. Their simulation results indicated that optimal timing of injection and different injection rates might be favorable to control the breakthrough of CO<sub>2</sub>. Khan *et al.*<sup>11</sup> performed numerical simulation to maximize enhanced gas recovery in a natural gas reservoir by storage of CO<sub>2</sub> and H<sub>2</sub>S. They concluded that CO<sub>2</sub> breakthrough at the production well occurred faster than the breakthrough of mixed CO<sub>2</sub>-H<sub>2</sub>S injection. Kühn *et al.*<sup>13</sup> carried out a comprehensive assessment of the EGR potential of the Altmark field and concluded that proper usage of storage capacity can mitigate the risk of leakage during EGR and CO<sub>2</sub> storage. Similarly, studies carried out on condensate gas reservoirs are emphasizing the potentials of these geological formations as a suitable site for CO<sub>2</sub> storage. For instance, Azin *et al.*<sup>16</sup> analyzed partial depleted gas reservoirs for CO<sub>2</sub> storage. They suggested a scheme for storage purposes by selecting an optimum pressure or injection of a high volume of gas at the early stage of injection for a suitable gas recovery. Barrufet *et al.*<sup>4</sup> evaluated the storage capacity of depleted condensate gas reservoirs and aquifers by considering formation types, level of CO<sub>2</sub> purity and injection schedules. They concluded that CO<sub>2</sub> injection recovers complete condensate which makes these reservoirs a

better place for storage compared to aquifers due to overall compressibility. Shen *et al.*<sup>18</sup> investigated CO<sub>2</sub> storage in nearly depleted gas reservoirs. They concluded that CO<sub>2</sub> sinks into the bottom of the gas cap and stores permanently when gas recovery by CO<sub>2</sub> displacement and condensate re-vaporization processes take place. Narinesingh and Alexander<sup>17</sup> showed that the injection pressure increases in high condensate recoveries due to the re-vaporization of the condensate drop-out. According to Yuan *et al.*<sup>19</sup>, a fast condensate recovery and CO<sub>2</sub> storage can be achieved by combining the processes of enhanced recovery and storage at the early stage of the field development.

Although the above studies confirmed the feasibility of dry and condensate gas reservoirs for CO<sub>2</sub> storage, there have been very limited number of researches assessing these reservoirs for sequestration. This might be due to the complexity of key storage aspects of these reservoirs such as injectivity, storage capacity, trapping mechanisms, and containment which have not been fully understood.<sup>20</sup> For instance, some gas reservoirs may cause loss of injectivity, over pressurization or less CO<sub>2</sub> immobilization as the mixture of CO<sub>2</sub> with the residual gas may change the properties of CO<sub>2</sub> and gas mixture.<sup>15, 18, 21-23</sup> In the meantime, CO<sub>2</sub> mixing with resident gas depends on reservoir geometry, anisotropy, heterogeneity, injection rate, time of injection, rock or fluid properties, and diffusion which can only be studied through numerical modeling. In this paper, a 3D numerical model was built for gas reservoirs based on the modified Peng-Robinson equation of state to explore their feasibility of a long-term CO<sub>2</sub> storage.

## **2. Methodology**

### **2.1 Numerical simulation**

Numerical simulations were performed by the help of Eclipse simulator which is an advanced industry standard finite difference flow simulator developed by Schlumberger Limited. It is a major tool used for compositional modeling of enhanced recovery processes and CO<sub>2</sub> storage. As mentioned earlier, injection after field depletion is the best scenario to sequester CO<sub>2</sub> with a better residual recovery.<sup>9, 17</sup> Hence, simulation was run for a long term-storage to investigate the compositional impact of different gas types on the storage of depleted gas reservoirs.

In the first step, compositions of dry, wet and condensate gas at the depleted stage were taken from the literature.<sup>22</sup> Adisoemarta *et al.*<sup>22</sup> used these compositions to calculate the compressibility factor for storage purposes in depleted gas reservoirs. In the data preparation stage by Adisoemarta *et al.*<sup>22</sup>, the hydrocarbon components were normalized to 1.0 mole and the components were analyzed to find the median composition for each category of gas reservoirs. Table 1 gives the normalized median compositions of each category of gas reservoirs used for the purpose of this study.

Table 1. Mole composition of typical reservoir fluids in depleted gas reservoirs expressed as the mole fraction of hydrocarbon components<sup>22</sup>

Components	Dry gas	Wet gas	Condensate (50psi)
<b>CO<sub>2</sub></b>	0.0001	0.0001	0.0001
<b>C<sub>1</sub></b>	0.9661	0.9002	0.2477
<b>C<sub>2</sub></b>	0.0267	0.0475	0.0527
<b>C<sub>3</sub></b>	0.0051	0.0203	0.0541
<b>C<sub>4</sub></b>	0.0020	0.0102	0.0770
<b>C<sub>5</sub></b>	0	0.0041	0.0667
<b>C<sub>6</sub></b>	0	0.0035	0.0734
<b>C<sub>7+</sub></b>	0	0.014	0.4282
<b>Total</b>	1	1	1

Dry gas has a significant concentration of methane (C<sub>1</sub>) whilst the wet and condensate gases have a remarkable amount of heptane's-plus fractions (C<sub>7+</sub>). There are no phase changes in dry and wet gases and, therefore, a median dry and wet gas compositions can be considered as the compositions of gas at depleted reservoir conditions. This, however, is not the case for retrograde gas, which undergoes a phase change at the reservoir condition. For the purpose of this study, depleted condensate gas compositions at the pressure of 50 psi was taken into consideration. This compositional gas data and the depletion pressure are favorable because the pore pressure depletion of gas reservoirs is large.<sup>24</sup>

Three different compositions representing three different gas types, as given in Table 1, were used to evaluate the suitability of gas reservoirs and describe the behavior of CO<sub>2</sub> once mixed with residual gases. A 0.0001 mole fraction from butane component of each gas was picked to introduce CO<sub>2</sub> in the modeling. The black oil PVT analysis by the PVTi module of Eclipse at the reservoir temperature of 220 °F was carried out to confirm the gas type and generate properties of each gas type including critical pressure, critical temperature, acentric factor together with z-factor and binary coefficients. These properties are essential inputs to govern the fluid properties for modeling the storage site. Figure 1 shows the phase diagrams of considered gases, which confirms the fluid type with reference to the temperature condition, position of critical point, and the envelop size as reported by McCain Jr<sup>2</sup> and Terry and Rogers<sup>3</sup>.

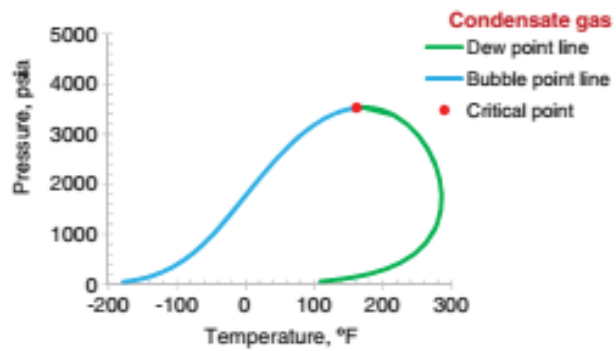
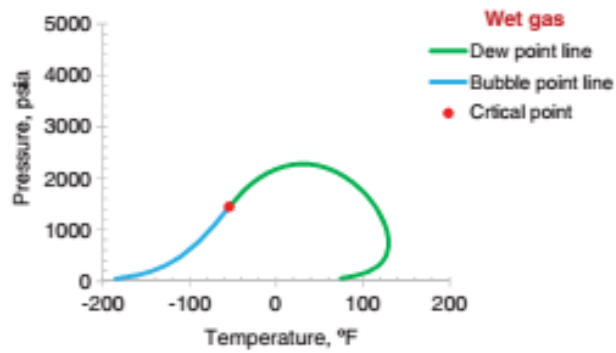
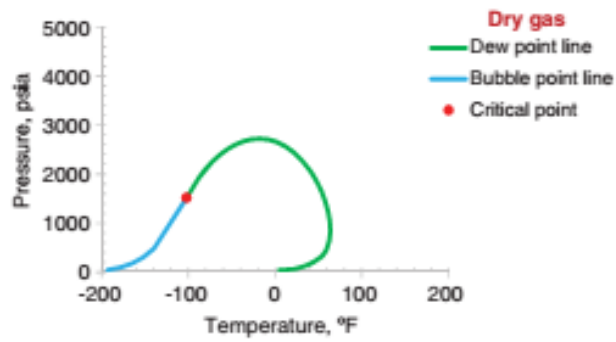


Figure 1. Phase diagram of dry gas (top), wet gas (middle) and condensate gas (bottom)

## 2.2 Modeling Approach

The GASWAT option of the Eclipse E300 simulator was used to model the storage of CO<sub>2</sub> in depleted gas reservoirs which is capable of solving the gas and brine phase equilibrium based on the adaptive implicit approach.<sup>8, 25, 26</sup> This method was applied to each gas type (dry, wet, and condensate) considering all essential parameters and modeling procedures. However, modeling the condensate liquid was not an easy task due to the limitation of GASWAT. As a result, modeling was solely done on the compositional effects (i.e., equilibrium between hydrocarbon rich and CO<sub>2</sub> rich phases) of different gas types on CO<sub>2</sub> storage. As a result, the total injected CO<sub>2</sub>, total stored CO<sub>2</sub>, and pressure buildup against time was predicted through this modeling.

In the modeling process, properties of gas, water and carbon dioxide (i.e., critical pressure, critical temperature, acentric factors and binary coefficients) were generated by the PVTi module of the Eclipse at reservoir conditions and CO<sub>2</sub> was separated for being traced individually. During simulation, solubility of CO<sub>2</sub> in water was determined by the Peng-Robinson Equation of State (PR-EOS) (see Eq. 1), according to the modification proposed by Soreide and Whitson.<sup>27</sup> Soreide and Whitson<sup>27</sup> modified the expression  $\alpha^{1/2}$  for the water component and expressed it by Eq. (2) which includes salinity ( $c_s$ ) of brine and reduced temperature,  $T_r$ , in the calculations. In fact, the Soreide and Whitson approach adds a temperature dependency behavior to the aqueous phase binary interaction coefficients. The solubility of gas was treated by the original Peng Robinson EOS.<sup>26</sup>

$$\left[ P + \frac{A}{V_M(V_M + B) + b(V_M - B)} \right] (V_M - B) = RT \quad (1)$$

In the above equation,  $P$  is the pressure (psia),  $V_M$  is the molar volume (cu ft/lb-mole),  $R$  is the gas constant (10.732 psia.cu.ft/lb. mole),  $T_r$  is the temperature (°F),  $A$  and  $B$  are the mixture-specific constants which are a function of temperature and composition. The coefficient  $A$  is defined based on the mole fraction, binary interaction coefficients, critical temperature and critical pressure.

$$\alpha^{\frac{1}{2}} = 1 + 0.4530 \left[ 1 - (1 - 0.0103c_s^{1.1}) T_r \right] + [0.0034(T_r^{-3} - 1)] \quad (2)$$

Although CO<sub>2</sub> displaces the resident gas by the miscible displacement process, and available gases will be mixed over time by the molecular diffusion, when the CO<sub>2</sub> diffusion coefficient at reservoir conditions is less than 10<sup>-6</sup> m<sup>2</sup>/sec, the effect of diffusion on the gas mixing and CO<sub>2</sub> dispersion can be ignored.<sup>7, 28</sup> Considering the importance of diffusion on the mixing, the

molecular diffusion was introduced and considered as part of the analysis.<sup>29-31</sup> This diffusion ensures that gas interblocks diffusive flows by defining the diffusivity input for each component<sup>25</sup> which is obtained using Eqs. (3) and (4)

$$J_i = -y \frac{D_i \partial y_i}{\partial d} \quad (3)$$

$$F_{ig}^{diff} = T_D D_{ig} (S_g b_g^m) \Delta y_i \quad (4)$$

In Eq. (3),  $x$  is the total molar concentration ( $\text{mol m}^{-3}$ ),  $J_i$  is the flux of component  $i$  per unit area ( $\text{mol m}^2 \text{s}^{-1}$ ),  $D_i$  is the diffusion coefficient of component  $i$  ( $\text{m}^2 \text{s}^{-1}$ ), and  $\partial y_i / \partial d$  is the molar concentration gradient of component  $i$  in the direction of flow (mole fraction). These diffusion coefficients are used in the simulator module to obtain the gas interblock diffusive flows expressed by Eq. (4). In Eq. (4),  $F_{ig}$  is the interblock diffusive flow ( $\text{mol}/\text{hour}$ ),  $T_D$  is the diffusivity ( $\text{m}^2/\text{s}$ ), and  $y_i$  is the vapor mole fractions,  $S_g$  is the gas saturation (fraction), and  $b_p^m$  is the molar density of gas ( $\text{mol}/\text{m}^3$ ).

The relative permeability of water and gas ( $\text{CO}_2$ ) was determined based on the approach presented by Oak.<sup>32</sup> The relative permeability curves obtained are shown in Figure 2, having 69% of initial gas saturation, 40% of trapped gas saturation and 31% of connate water saturation. It was then apparent that hysteresis effects are strong in the gas relative permeability only. One may say that these data were generated for a brine-nitrogen gas system under a low pore pressure condition<sup>32</sup> and may not be suitable for a  $\text{CO}_2$  system. It should be noted that this data has already been used to study the hysteresis of relative permeability in saline aquifers<sup>33</sup>, and the value of residual gas saturation at 40% is within the range of experimental values presented by Bennion and Bachu.<sup>35</sup> GASWAT modeling is used in order to model gas ( $\text{CO}_2$ )/aqueous phase equilibria for  $\text{CO}_2$  storage in depleted gas reservoirs by utilizing the relative permeability and capillary pressure data of water and gas ( $\text{CO}_2$ ) phases. Pure  $\text{CO}_2$  injection was made in water zone. Considering this facts, combinations of gas and water relative permeability of  $\text{CO}_2$  injection in aquifer which are taken from Juanes et al., 2006 was utilized to quantify the effect of different gas type in residual form on  $\text{CO}_2$  storage performance.

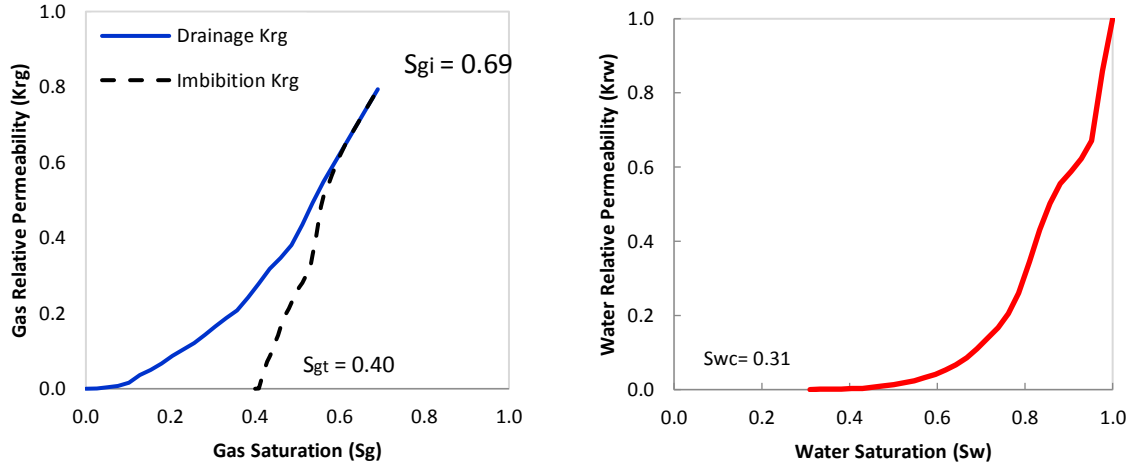


Figure 2. Relative permeability curves used in the CO<sub>2</sub> simulations, generated from the data by Oak.<sup>32</sup> for a water-wet Berea sandstone<sup>33</sup>.

The most important parameter quantifying the significance of hysteresis is the trapped gas saturation ( $S_{gt}$ ) after a flow reversal (from drainage to imbibition), which can be used to relate trapped (residual) gas saturation to the maximum gas saturation ( $S_{g,max}$ ). The common relative permeability hysteresis models often used for the trapping modelling is the one proposed by Land.<sup>36</sup>, which formulates the Land Model as given in Eqs (5-6).

$$S_{gt} = \frac{S_{gi}}{1 + CS_{gi}} \quad (5)$$

Where

$$C = \frac{1}{S_{gt,max}} - \frac{1}{S_{g,max}} \quad (6)$$

In this model,  $S_{gi}$  is the initial gas saturation at the flow reversal and  $C$  is the Land trapping coefficient computed from the bounding drainage and imbibition relative permeability curves. The bounding drainage and imbibition curves obtained from the experimental data indicated that the Land trapping coefficient,  $C$ , can be approximately equal to 1.  $S_{gt,max}$  is the maximum trapped gas saturation linked to the imbibition curve where  $S_{g,max}$  is the maximum gas saturation.

Capillary forces and relative permeability affects will contribute in residual trapping<sup>36</sup>. According to Spiteri and Juanes.<sup>34</sup>, capillary pressure effects are negligible during numerically simulating field-scale displacements in case, when the characteristic capillary length is much smaller than the grid resolution. Juanes et al.<sup>33</sup> also found that their numerical predictions are insensitive to the options of the hysteretic or nonhysteretic capillary pressure curves, while emphasized on accounting CO<sub>2</sub> trapping in the relative permeability model for

evaluation of the distribution and mobility of CO<sub>2</sub> in the formation.<sup>33</sup> Thus, we assumed ignored capillary pressure data in the simulations presented here.

A relative permeability hysteresis model characterizes the scanning curves during imbibition and drainage cycles. In this paper, the hysteresis model developed by Killough.<sup>37</sup>, were utilized in which the gas relative permeability along a scanning curve, such as the one shown in Figure 3 is determined by using the expression given in Eqs (7,8). For a given value of S<sub>g,max</sub>, the trapped critical saturation and the relative permeability for a particular gas saturation, S<sub>g</sub>, on the scanning curve is calculated by using the expression given in Eqs. (7-8).<sup>33</sup>

$$k_{rg}^i(S_g) = k_{rg}^{ib}(S_g^*) \frac{k_{rg}^d(S_{gi})}{k_{rg}^d(S_{gi,max})} \quad (7)$$

Where,

$$S_g^* = S_{gt,max} + \frac{(S_g - S_{gt})(S_{gi,max} - S_{gt,max})}{S_{gi} - S_{gt}} \quad (8)$$

In the above equations, k<sub>rg</sub><sup>d</sup> and k<sub>rg</sub><sup>ib</sup> represent the bounding drainage and imbibition curves, respectively. S<sub>g,max</sub> is the maximum gas saturation, and S<sub>gt,max</sub> is the maximum trapped saturation, associated with the bounding imbibition curve.

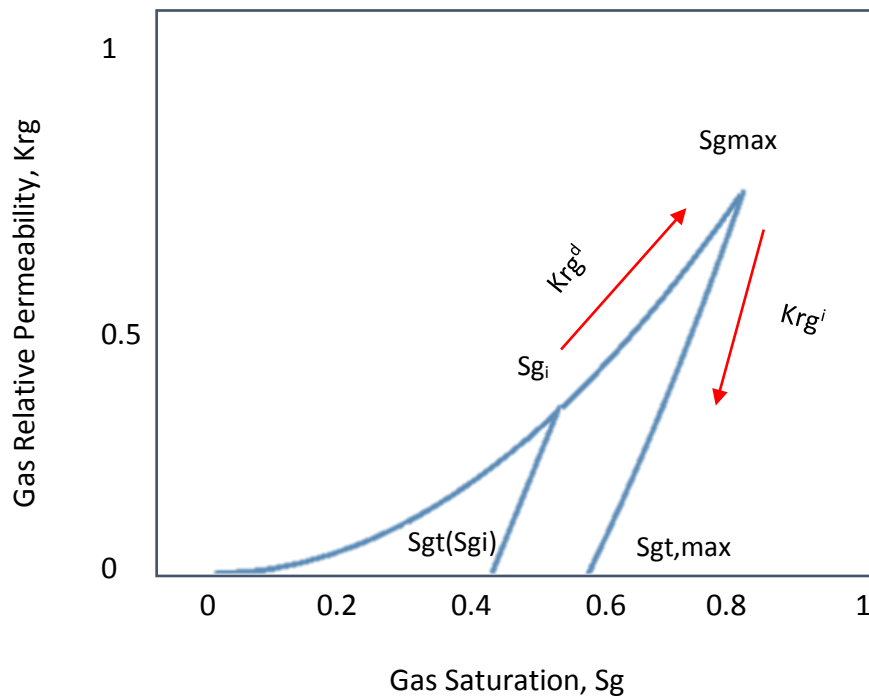


Figure 3. Parameters involved in the evaluation of the Land Trapping model<sup>33</sup>

### 2.3. Model Description

In view of huge time required for running a three-dimensional simulation, a 3D Egg model was utilized for evaluating the long-term injection of CO<sub>2</sub> into dry, wet and condensate gas reservoirs. The "Egg Model", is a synthetic static reservoir model consisting of an ensemble of 101 relatively small three-dimensional permeability realizations,<sup>38</sup> built by considering three permeability realizations. The grid dimension of the model was modified from the smaller to bigger size going up to 3937 ft in a horizontal XY plane with a thickness of 200 ft (i.e., 7 layers) for a thorough evaluation of heterogeneity,<sup>39, 40</sup> time-scale of convective mixing, plume size and degree of CO<sub>2</sub> stored.<sup>41</sup> To ensure the presence of supercritical CO<sub>2</sub>, the top depth of the first layer out of seven layers was set at 13000 ft. However, zero dip angle considered to neglect the effect of gravity segregation. Water was also present at the gas-water contact depth of 13190 ft. A single injection well was located in middle grid and perforated in last three layers to make pure CO<sub>2</sub> injection in water phase at a rate of 100MScf/day. However, major portion was occupied by residual gas phase which would help to quantify the effect of different gas type on CO<sub>2</sub> storage. The lateral boundaries are at average distance of from the injection well to have impact on the CO<sub>2</sub> plume evolution.

The model had a porosity and channel permeability of 0.30 and 800 mD, respectively. The permeability in XYZ directions was similar (isotropic). Figure 4 displays the permeability distribution in the model where the X-Y plane has 3600 grid blocks in each direction. The major portion of the model had a low matrix permeability (40 mD) with a high permeability meandering channels in unconsolidated sandstone layers. This high heterogeneity would help to evaluate the gas mixing as heterogeneity and reservoir aspect ratio directly affect the mixing<sup>42</sup> while low permeability is an important factor to enhance hysteresis and capillary effects.<sup>43, 44</sup> This model description used in link with generated PVT data for different gas types to evaluate CO<sub>2</sub> storage performance. Details of the properties and parameters used in the model are listed in Table 2.

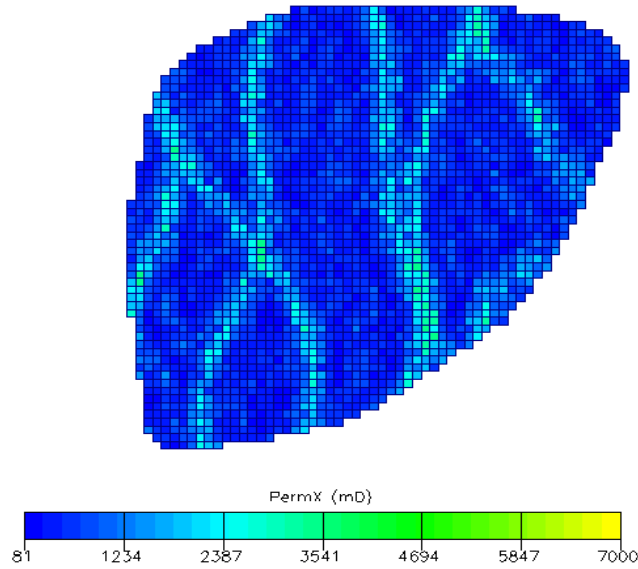


Figure 4: Top view of the egg shaped reservoir model displaying a typical structure of high-permeability meandering channels (800 mD) in a low permeability blue background matrix (<40 mD)

Table 2: Reservoir and fluid properties used in this study

Symbol	Variable	Value	Field Units	
N	Grid blocks	25200		
	Active blocks	18553		
L	Length	1200	feet	
W	Width	1200	feet	
H	Thickness	200	feet	
D <sub>top</sub>	Depth at the top of the injection well	13000	feet	
α	Dip degree	0		
φ	porosity	30	%	
K	Channel permeability	800	mD	
D	Molar concentration gradient of component	CO <sub>2</sub>	1.72 10 <sup>-5</sup>	m <sup>2</sup> /sec
		C <sub>1</sub>	1.61 10 <sup>-5</sup>	
		C <sub>2</sub>	4.30 10 <sup>-6</sup>	
		C <sub>3</sub>	4.30 10 <sup>-6</sup>	
		C <sub>4</sub>	4.30 10 <sup>-6</sup>	
		C <sub>5</sub>	4.30 10 <sup>-6</sup>	
		C <sub>6</sub>	1.20 10 <sup>-5</sup>	
		C <sub>7+</sub>	1.40 10 <sup>-6</sup>	
	Liquid	10 <sup>-10</sup>		
Cr	Rock compressibility	2×10 <sup>-7</sup>		
S <sub>wc</sub>	Connate water saturation	31	%	
P <sub>ini</sub>	Initial reservoir pressure	50	psi	
S	Salinity	15000	ppm	
Temp	Temperature	220	°F	
Q <sub>g</sub>	Gas injection rate	100	MScf/day	
S	Skin	0		
PV	Initial pore volume	6.6	Billion tons (Bt)	
xCO <sub>2</sub>	CO <sub>2</sub> mole fraction	1	Mole fraction	
P <sub>max(inj)</sub>	Maximum injection pressure	4500	psi	
T	Injection time	5	years	
	Simulation time	1000	years	

## **2.4. Initial conditions for simulation**

During the simulation, the volumetric gas reservoir was assumed to be at the end of the gas production. There were only brine and gas phases in the reservoir before CO<sub>2</sub> injection having pressure of 50 psi and a gas-water contact at a particular datum depth of 13150 ft. The temperature was assigned to be 220 °F, while the initial gas saturation at the depleted stage for dry, wet and condensate gas cases were respectively 0.19, 0.14, 0.11 fractions. Prior to CO<sub>2</sub> injection, the remaining gas at the depleted condition pressure of 50 psi was different in various media. Thus, relative permeability data for residual gas phase is not required by GASWAT module. During injection phase, drainage relative permeability data of CO<sub>2</sub> and water phases is used as injection is a drainage process. At the time of storage process, imbibition relative permeability data of CO<sub>2</sub> and water phases is acquired by GASWAT module. Therefore, significant residual trapping is occurred after injection stops when water displaces CO<sub>2</sub>.<sup>33</sup> Owing to this, relative permeability hysteresis data by Juanes et al. (2006)<sup>33</sup> accounting for CO<sub>2</sub> trapping was considered for predicting the distribution and mobility of CO<sub>2</sub> in the formation after injection stops. A well was considered for the injection of pure CO<sub>2</sub> (i.e., 100 mole percent of CO<sub>2</sub>) under a maximum sustainable pressure of 4500 psi at a rate of 100MScf/day for 5 years. A skin equal to zero was considered near the well bore of the injection well. To investigate the long-term storage of CO<sub>2</sub> in the gas reservoirs, the simulation was run for 1000 years.

## **3. Results and Discussions**

Quantifications of the storage aspects for formation reservoirs with different gas compositions at particular conditions was evaluated in this study. Considering the simulation conducted, it can be safely say that the results obtained are realistic since the actual protocol adopted to carry out the simulation covers all possible factors included in the realistic modeling of dry, wet and condensate gases compositions.

In order to investigate the interaction between different kinds of gases and CO<sub>2</sub>, three simulation cases were generated and named as dry-base, wet-base and condensate-base. Moreover, the effect of the injection rate and heterogeneity during storage was also evaluated. These three cases are neglecting the CO<sub>2</sub>-water-rock reaction for precipitation and dissolution during injection due to the limitation of the simulator<sup>25</sup> and low reactivity of sandstone reservoirs.<sup>45</sup>

### **3.1. Temporal evolution of CO<sub>2</sub> in different phases**

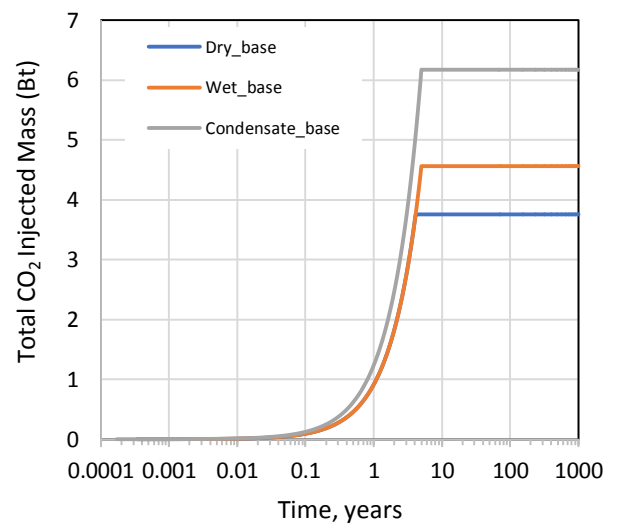
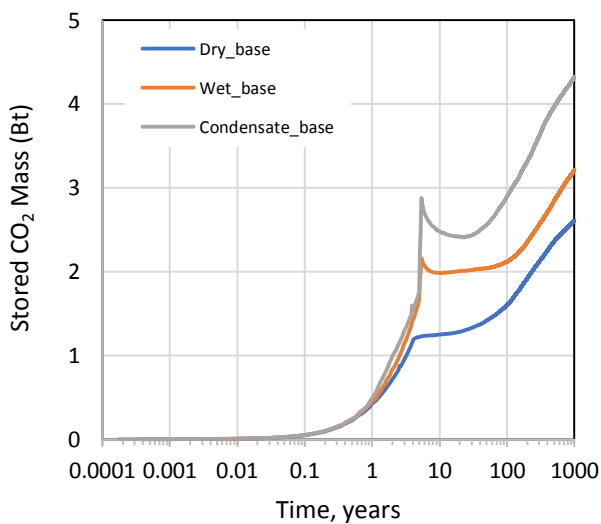
As mentioned earlier, there are four major trapping mechanisms for CO<sub>2</sub> storage in a gas reservoir. When CO<sub>2</sub> is injected into a gas reservoir, initially displaces the brine and gas, mixes with the resident gas and flows upwards by the buoyant force because it is less dense than water. During this process, a fraction of CO<sub>2</sub> is capillary trapped as the residual CO<sub>2</sub> saturation in narrow pore throats in a short-term scale. In a longer term, a significant amount of CO<sub>2</sub> dissolves in brine and forms an immobilized dissolved phase. The dissolved CO<sub>2</sub> can form H<sub>2</sub>CO<sub>3</sub>(aq), HCO<sub>3</sub><sup>-</sup>, and CO<sub>3</sub><sup>2-</sup> by interacting with brine which can change the pore geometry due to the dissolution and precipitation of minerals in the reservoir. Some fractions of CO<sub>2</sub>

are also transformed into stable carbonate minerals (mineral phase) for the permanent storage, but this mechanism was not taken into consideration during simulation by GASWAT E300. During and after injection, trapping mechanisms play their role to store (immobilize) the injected CO<sub>2</sub>, depending on the characteristics of the storage medium.<sup>46</sup> Figure 5 (a) indicates that the mass of CO<sub>2</sub> storage in different gas mediums start to increase slowly till the injection period of 5 years which is aligned with earlier study<sup>47</sup>. Once injection stops, mass of CO<sub>2</sub> stored due to the residual and dissolution trappings starts to decline for few years, but sharply increases after that. Figure 5 (a) confirms that that the residual trapping and dissolution trapping play crucial roles to achieve a favorable CO<sub>2</sub> storage capacity. Condensate gas, which has the maximum residual and dissolved CO<sub>2</sub> saturations, shows the maximum storage capacity during and after injection as discussed earlier<sup>22</sup> Comparison of the dry base, wet base, and the condensate base cases shows that the storage medium with condensate gas has significant impact on the total storage capacity due to favorable residual and dissolution trapping. This may indicate that high a compressible fluid like condensate gas is favorable to immobilize large fraction of CO<sub>2</sub> in the form of residual and dissolved phases. Comparing the total injected mass of CO<sub>2</sub> in Figure.5 (b), it can be seen that that the maximum mass of CO<sub>2</sub> was injected in the condensate base case and the least amount belongs to the dry base case. The total amount of injected CO<sub>2</sub> in all three cases was different ranging from 3.75 billion tonnes (Bt), 4.50 Bt, and 6.16 Bt for dry, wet and condensate base cases respectively owing to the effect of the bottom-hole injection pressure and pressure distribution in the reservoir. It seems that condensate gas with a lower remaining gas at the depleted pressure would be more beneficial for enhancing the well injectivity by permitting more CO<sub>2</sub> to flow into the reservoir. It might be due to the high compressibility of condensate gas at the depleted stage compared to dry and wet gases because condensate gas at 50 psi is 1.1 times more compressible than condensate at 500 psi for wet and dry gases.<sup>23</sup>

The pressure buildup due to CO<sub>2</sub> injection is generally not a limiting parameter but must not exceed the fracture initiation pressure of formations.<sup>47</sup> In this study, the maximum injection pressure was monitored in dry, wet and condensate gas media upon injection as shown in Figure 5(c). Looking at this figure, it can be concluded that the pressure reaches its maximum value in the dry base case but stays at its lowest magnitude in the condensate base case regardless of the huge mass of CO<sub>2</sub> which was injected and stored in the condensate gas formation. This behavior of pressure in different gas mediums can be attributed to the compressibility level of these gases. Figures 6 shows the percentage of CO<sub>2</sub> in different phases over time for all three cases of gas reservoirs.

As it is seen in this Figure, initially a large amount of CO<sub>2</sub> resides in the reservoir, while some amounts are residually trapped and dissolved at the early stage of injection. As injection continuous, the amount of supercritical CO<sub>2</sub> increases at the end of injection after 5 years in which 38.2%, 42.5% and 65% of CO<sub>2</sub> is trapped in dry, wet and condensate cases, respectively. Residual and dissolved trapping are not significant and within the range of 8-20% in a short-term geological sequestration of CO<sub>2</sub>. Moreover, the potential of residual phase trapping is less than the dissolution in the base case of wet and condensate gases for a short-term

scenario. As time passes, the capillary phenomenon becomes significant resulting in the increase of residual phase while dissolution takes place with a slow rate, enhancing CO<sub>2</sub> residual trapping and dissolution in brine. On the other hand, CO<sub>2</sub> in the supercritical phase is reduced as time passes. At the end of 1000 years, the residual trapping becomes the main mechanism of trapping and more than half of total CO<sub>2</sub> injected is trapped. In a short or long term scenario, the amount of supercritical CO<sub>2</sub> is significant in the condensate gas medium while it is very minor in a dry gas reservoir. However, all gas types show a great potential for residual trapping relative to dissolution trapping in a long-term and the free CO<sub>2</sub> phase is residually trapped and decrease with time. Comparatively, the condensate gas reservoir offers a significant immobilization in residual and dissolution phases (65.2%) during shut-in period till 1000 years. Nevertheless, the pressure and molecular diffusivity play a major role in the gas mixing, which can be attributed to the interactions of CO<sub>2</sub> with gas components and remaining gas saturation as explained earlier. It was also revealed that components other than methane might enhance the residual and dissolution mechanisms as methane solely support more dissolution compared to CO<sub>2</sub>, O<sub>2</sub>, SO<sub>2</sub>, H<sub>2</sub>S, and N<sub>2</sub>.<sup>49</sup> However, the dry base case doesn't show any significant dissolution trapping even in the presence of high huge methane. Although, the high percentage of supercritical phase in condensate base case relative to others is a favorable option for injection and storage, it may initiate leakage due to its long term contact with the caprock<sup>50, 51</sup>. Table 3 summarizes the material balances (total injected CO<sub>2</sub>, stored CO<sub>2</sub> and maximum pressure buildup) of dry base, wet base, and condensate base cases.



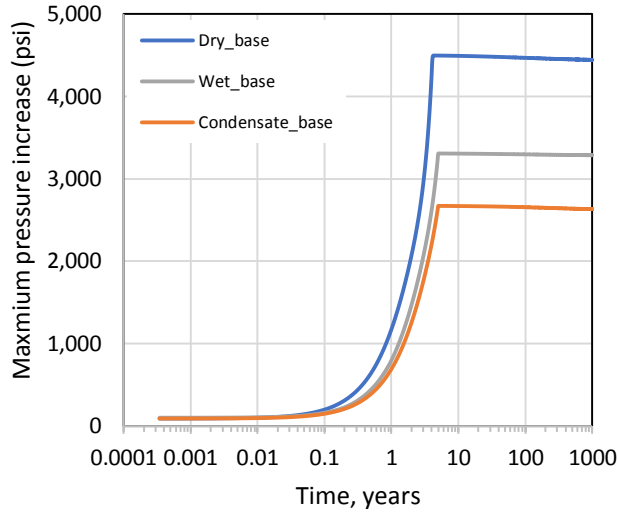


Figure 5. (a) Comparison of gas mediums for total mass of CO<sub>2</sub> stored at different time intervals; (b) The total injected CO<sub>2</sub> mass vs time; (c) The maximum pressure buildup vs time

Generally, the condensate gas type has a high compressibility and as such it offers a larger storage capacity compared to dry and wet gas type<sup>22, 23</sup> as also evident in Figure 6. A similar conclusion was made by Sobers *et al.*<sup>23</sup>, where the large storage capacity of condensate gas reservoirs was attributed to the phase behavior of the condensate gas-CO<sub>2</sub> mixture<sup>23</sup>, good injectivity due to a high compressibility, low remaining gas, and small amount of methane mole fractions. Although the effect of the condensate liquid was not included in the analysis of this study due to the limitation of GASWAT, it seems that it could further enhance the storage space<sup>23</sup> and recovery by re-vaporization.<sup>17</sup>

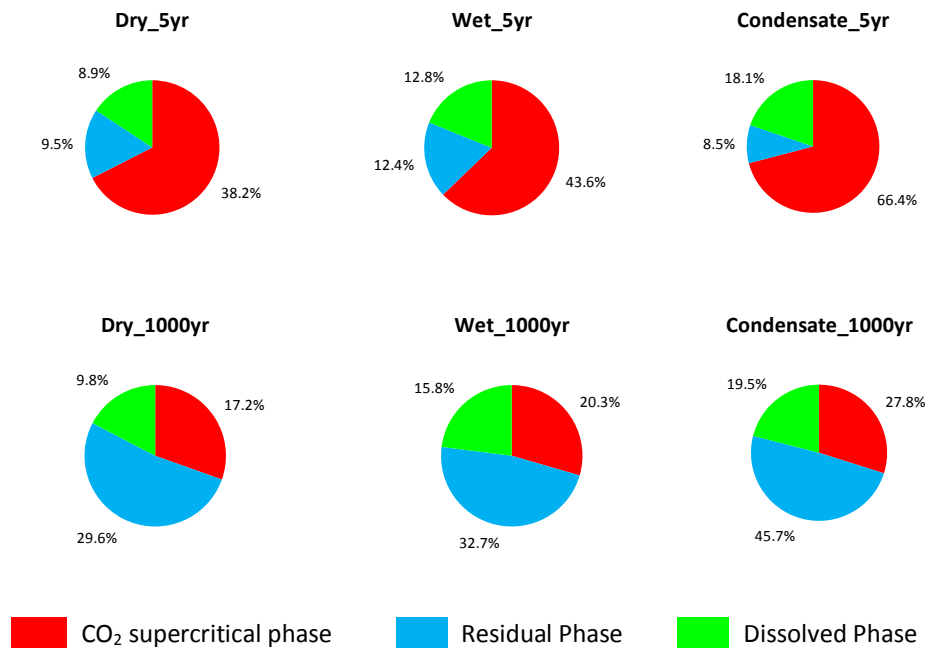


Figure 6. Percentage of CO<sub>2</sub> in different phases after 5 years and 1000 years in dry gas, wet gas and condensate gas reservoirs

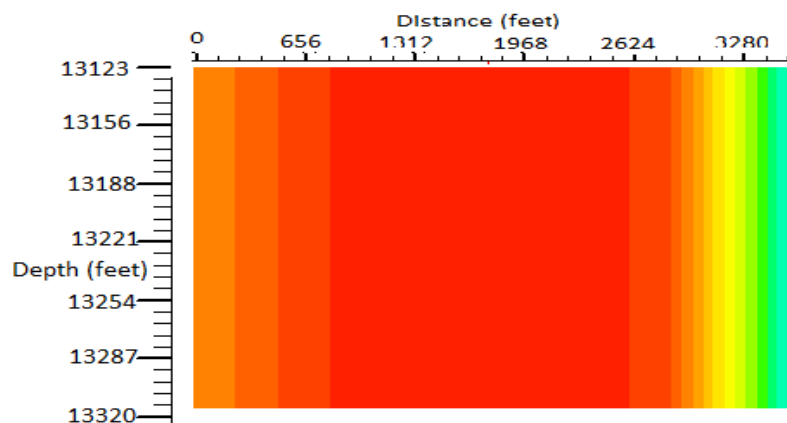
Table 3: Summary of the gas type effect on cumulative injected CO<sub>2</sub>, total stored CO<sub>2</sub>, and maximum pressure buildup

Case	Gas Type	CONSTRAINTS		Inj. Rate (MScf/D)	Cum. CO <sub>2</sub> Injected (Bt)	CO <sub>2</sub> amount in 1000 years (Bt)			Maximum pressure buildup, psi
		BHP (psia)	Inj. Time (years)			Supercritical free phase	Stored CO <sub>2</sub> as Residual phase	Stored CO <sub>2</sub> as Dissolved in brine	
Base	Dry	5000	5	100	3.75	1.14	1.96	0.65	4496
Case	Wet	5000	5	100	4.55	1.34	2.16	1.05	3307
	Condensate	5000	5	100	6.16	1.84	3.03	1.29	2671

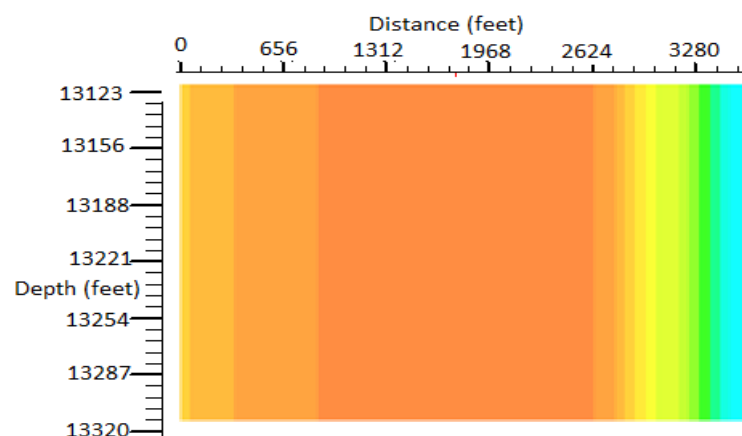
### 3.2. Spatial evolution of CO<sub>2</sub> mixing

Pressure built up near the injection well was expected during injection, resulting in generation of a high saturation region near the wellbore which smoothly depleted towards the reservoir. This build-up slowly decreases after the stoppage of injection in 5 years for all base cases (dry, wet, condensate), although gas mixing may play an important role in this reduction. According to Oldenburg<sup>28</sup>, gas mixing in the medium increases with pressure, which depend on rock and fluid properties, may result in different compositions of CO<sub>2</sub> phases. This is clearly observed in Figures 7 and 8 which are demonstrating the maximum pressure build up near the injection well and CO<sub>2</sub> saturation in the reservoir, respectively. Overall, the results obtained from saturation and pressure build up are aligned with what was shown in Figure 5. Figure 9 shows the distribution of CO<sub>2</sub> mixed with gas in the top layer of the model for all three cases after 5 and 1000 years.

Dry base



Wet base



Condensate base

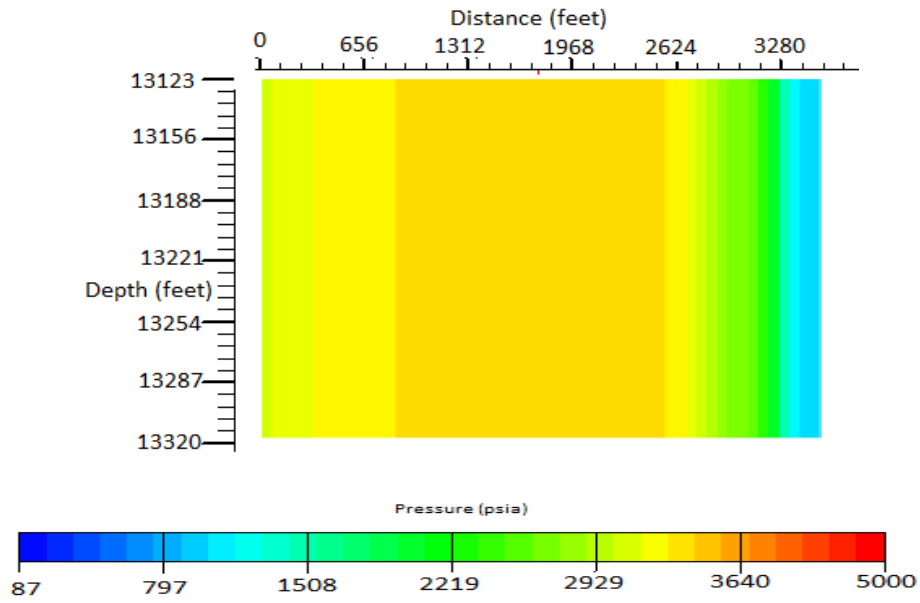
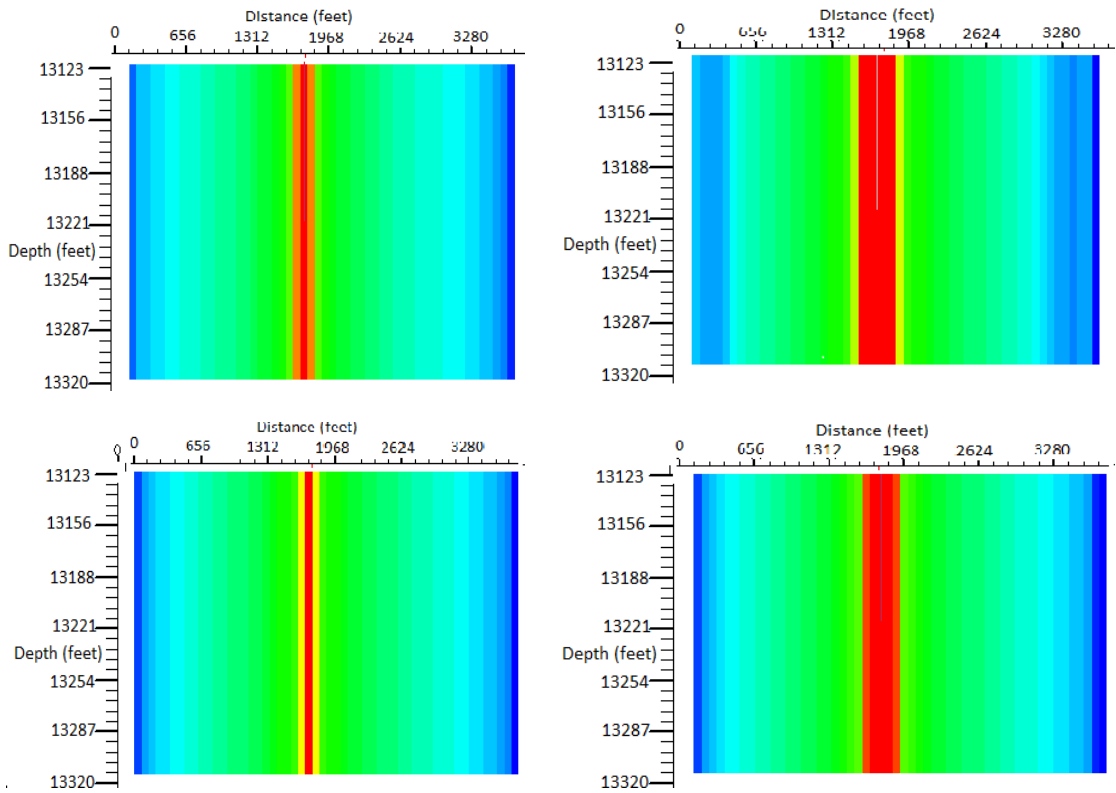


Figure 7. Cross section view of the reservoir for maximum pressure build at the end of 1000 years near the wellbore in dry base, wet base, and condensate base cases



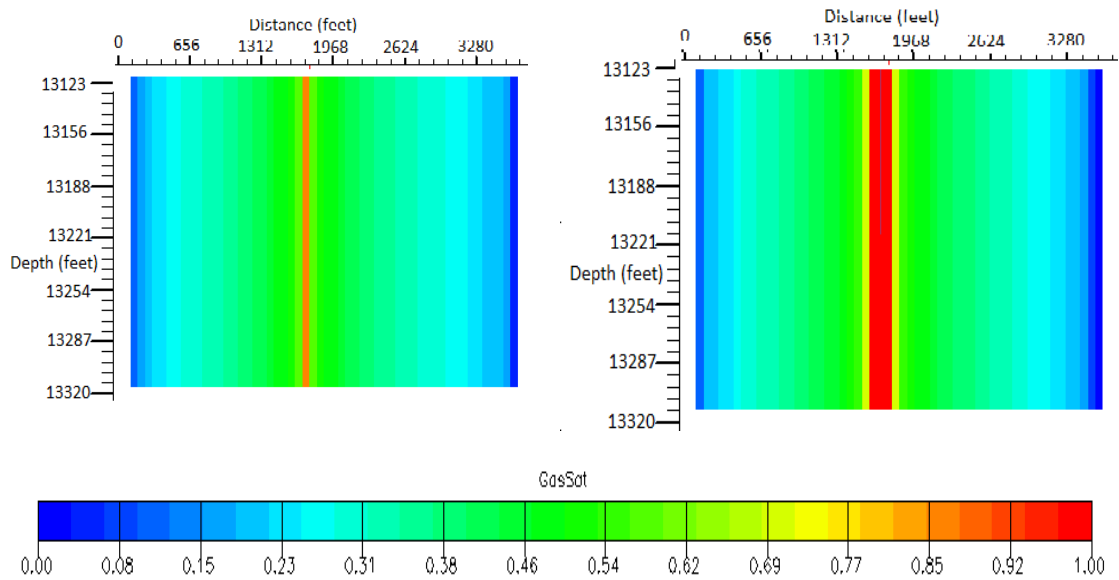
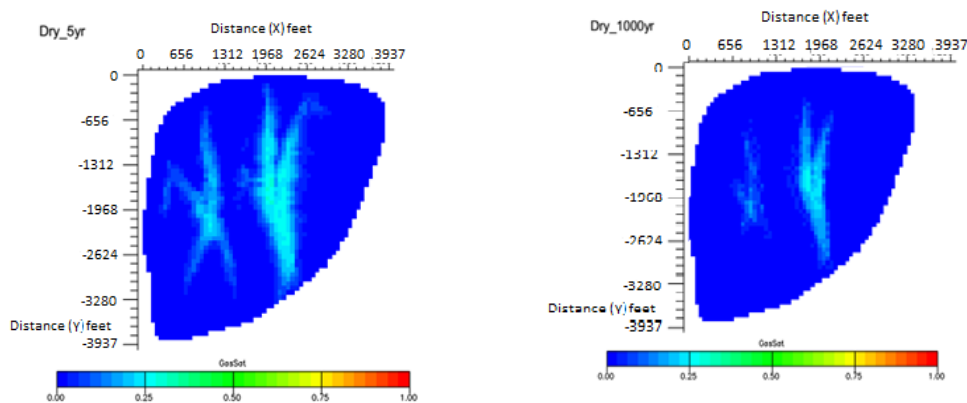


Figure 8. Cross section view of the reservoir for CO<sub>2</sub> saturation distribution near the wellbore in the dry base (top), wet base (middle), and condensate base (bottom) cases after 5 years (left) and 1000 years (right) of storage. Red strip shows the high gas saturation near the wellbore

The contours shown in Figures 8 and 9 indicates that once injected, CO<sub>2</sub> quickly moves away from the injection site into the high permeable area and slowly spreads into the surrounding low permeable portions. The fraction in the blue zone is very small after displacing the remaining gas during the first 5 years in all three base cases. During the whole process in three cases, the low permeable and high heterogeneous areas are holding a low saturation over a short to long term period of time.



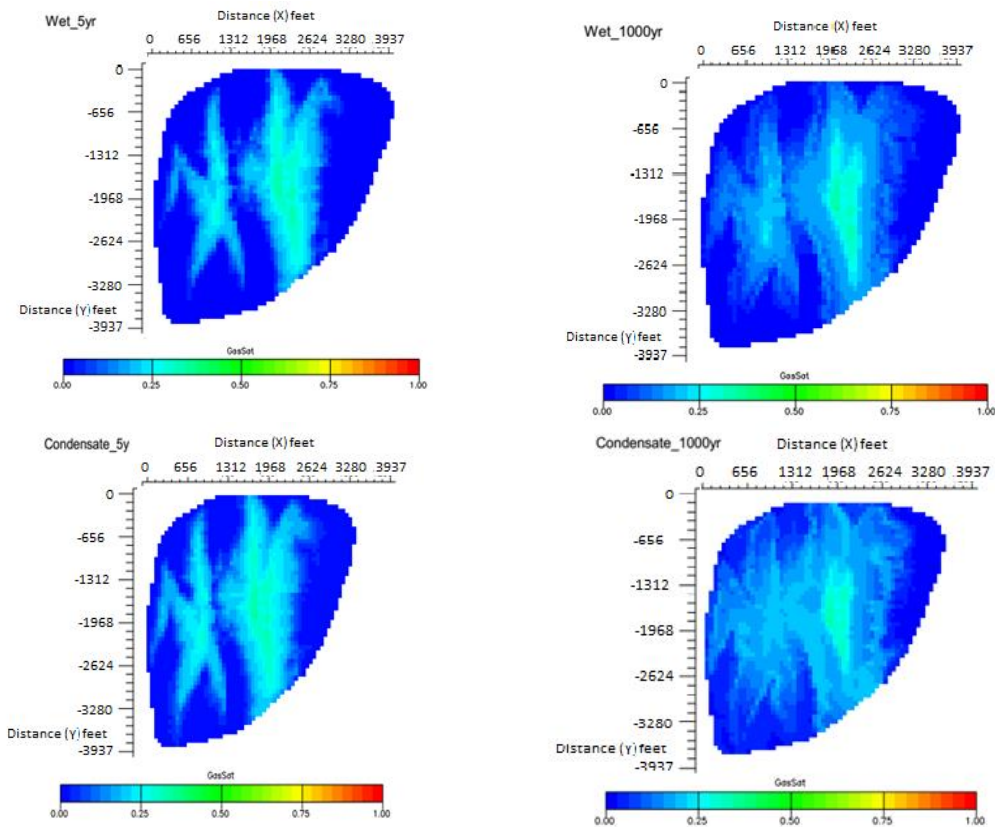


Figure. 9: CO<sub>2</sub>-gas distribution in k=1 at 5 years (well shut-in time), and 1000 years for dry gas, wet gas and condensate gas

On the other hand, the spatial distribution of gas-CO<sub>2</sub> saturation in the high permeable channels is high. Comparatively, the total gas saturation including remaining gas and CO<sub>2</sub> supercritical phase after 5 years is huge which starts to decrease as we get closer to 1000 years. The same phenomenon was observed in the dry and wet gas reservoirs over a short to long term period. However, the thermal and capillary effects posed after injection on the caprock integrity<sup>52</sup> in these types of gas reservoirs must be evaluated before getting any further conclusions.

#### 4. Sensitivity analysis

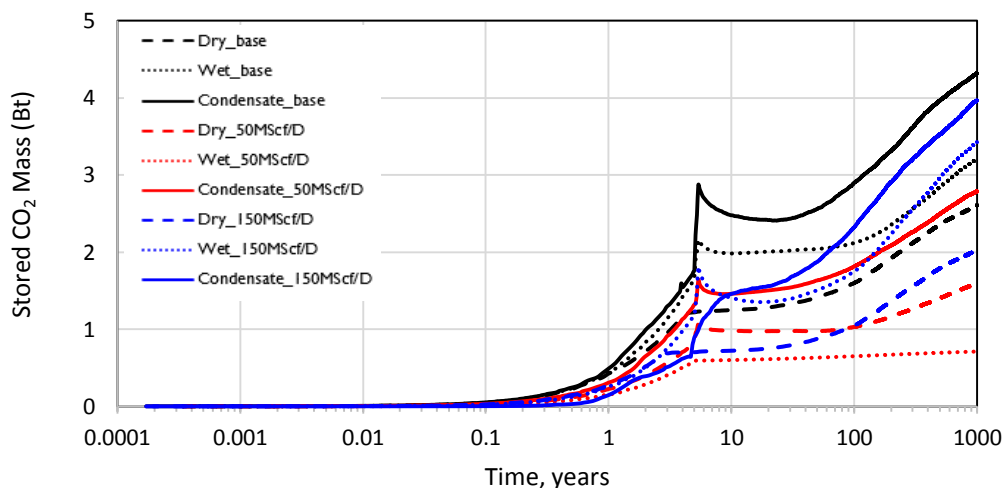
The model built in this study was based on three types of gas compositions which may have different impacts on the mechanism of CO<sub>2</sub> storage, but there are few important parameters such as injection rate and heterogeneity which may vary from case to case, offering different storage potential for the rese upon injection. In this section, these two parameters were evaluated and their impacts on the overall performance of the gas reservoirs were reported.

##### 4.1. Injection Rate

Injection rate plays an important role in achieving a desired CO<sub>2</sub> volume and having a certain mixture of CO<sub>2</sub> with gas. However, it should be noted that in gas reservoirs, injectivity might be affected by the presence of the residual gas (methane).<sup>28, 53</sup> There have been many studies in which trapping mechanisms, especially capillary trapping, suppressed at a high injection

rate.<sup>54-57</sup> Considering these facts, a low (50 MScf/D) and high injection rates (150 MScf/D) were selected and compared to evaluate different gas reservoirs against the variation of injection rate. The results obtained from running the numerical model for 5 and 1000 years indicated that at a low injection rate of 50MScf/D, the storage capacity of the dry gas medium is more than the wet gas case but less than the condensate gas system. The storage potential of the dry gas reservoir at the high injection rate seems to be the lowest and that of the condensate gas would be the highest similar to the base case. Thus, it was concluded that storage potential is sensitive to the gas type. At different rates, the condensate gas medium shows a high potential compared to other two cases if the mass of CO<sub>2</sub> stored is compared. This highlights the fact that an optimum injection rate may help to achieve a good capacity in condensate gas systems. Figure 10a shows the amount of CO<sub>2</sub> stored in different gas reservoirs at low and high injection rates.

As it is seen in Figure 10b, the total amount of CO<sub>2</sub> injected increases gradually at early stages (after 5 years) and stabilized once injection stops. However, the total injected CO<sub>2</sub> is low in the dry and wet gas systems compared to the condensate gas medium at the low injection rate. A very similar trend exists at the high injection rate, but the amount of CO<sub>2</sub> injected was clearly lower than the low injection rate as shown in Figure 10b. It worth to mention that a large amount of CO<sub>2</sub> is injected at a high injection rate in the wet and condensate gas cases compared to the wet base and the condensate base cases. On the contrary (see Figure 10a), lesser amount of CO<sub>2</sub> was stored in these two gas systems through residual and dissolution trappings at the high injection rate of 150 MScf/D compared to the results obtained from the injection rate of 100 MScf/D. This might be related to the effect of high injection rate which suppresses the residual trapping and dissolution trapping potentials<sup>55,56</sup> and as such a huge amount of CO<sub>2</sub> appears under supercritical condition.



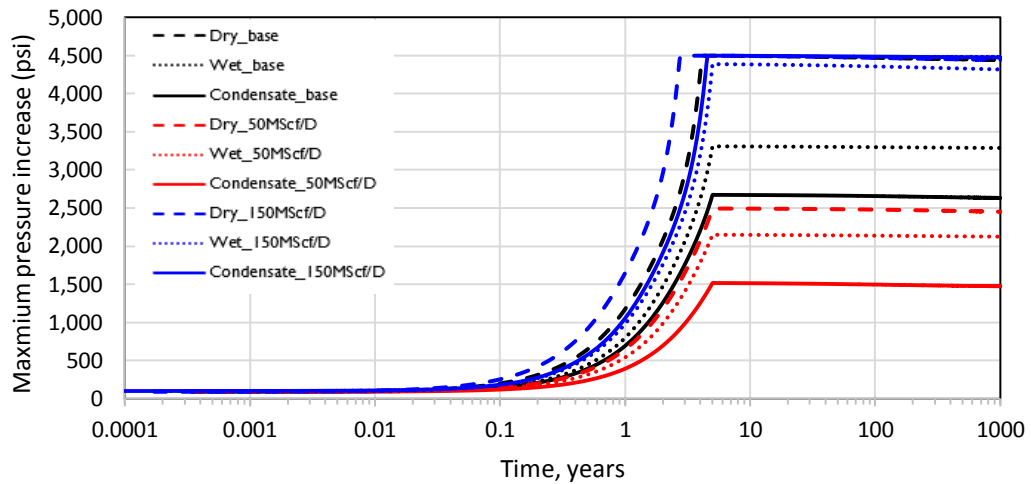
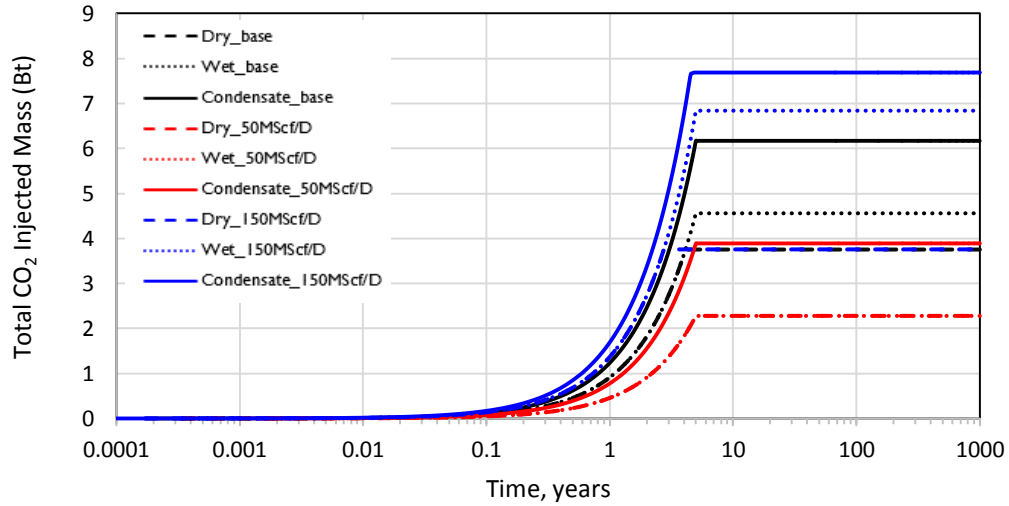


Figure. 10: (a) Comparison of gas mediums for total mass of CO<sub>2</sub> stored at different time; (b) The total injected CO<sub>2</sub> mass vs time; (c) The maximum pressure buildup vs time at different injection rates (50 MScf/D, 100 MScf/D and 150 MScf/D)

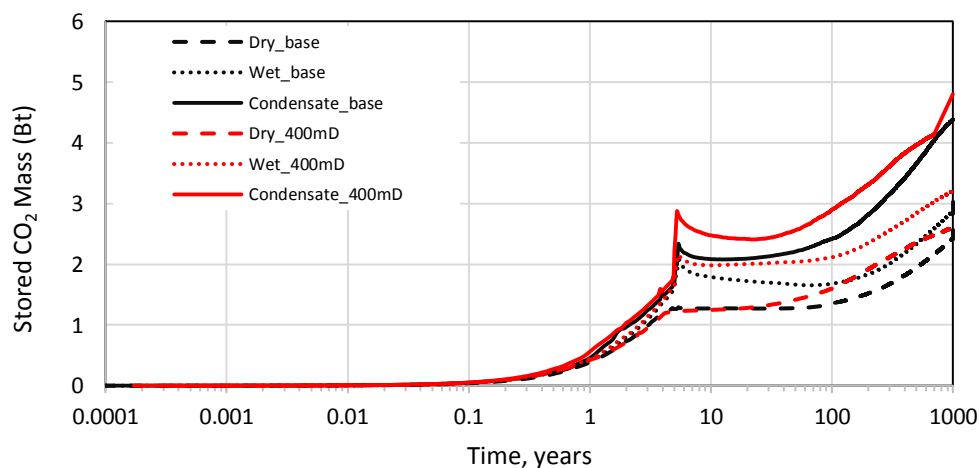
It was also found that the trends of pressure build up in the gas mediums slowly increases up until the end of injection periods<sup>47</sup>, regardless of injection rate chosen. The trend of pressure increase in at a low injection rate is similar but quantitatively less than the one observed in bases cases. The most important observation was the pressure build up at a high injection rate which was maximum for all gas formations approaching to the pressure build up observed at 5 years in the dry base case (see Figure 10c). Thus, it could be concluded that selection of an appropriate gas medium plays an important role to achieve a favorable storage potential with lesser mobile CO<sub>2</sub> and lower pressure build up.

#### 4.2. Heterogeneity

Heterogeneity may have impacts on the multiphase flow of CO<sub>2</sub>-brine<sup>58</sup> and can be expressed in terms of permeability variation.<sup>28</sup> The storage capacity is linked to heterogeneities and porosity, whilst injectivity is related to petrophysical properties such as permeability.<sup>59</sup> To

analyze the effect of permeability, numerical simulation was run by considering the channel permeability of 400 mD by multiplying reduction factor to the base cases (dry, wet and condensate). The results obtained which are shown in Figure 11a revealed that the trends of CO<sub>2</sub> storage through residual and dissolution trappings is quantitatively similar to the trends of the bases case in all gas systems up until the end of the injection period. Once injection stops, the amount of CO<sub>2</sub> stored in the case with the permeability of 400 mD gradually increased and becomes more than that of the base case for all gas systems due to favorable residual and dissolution trappings as reported in Table 4. The total amount of storage in dry, wet, and condensate gas mediums was around 2.87 Bt, 3.37 Bt, and 4.80 Bt, respectively after 1000 years. This increase in the amount of CO<sub>2</sub> storage after injection in the channel permeability case could be related to hysteresis and capillary effects which are changed by the variation of permeability.<sup>43, 44</sup>

The results of total injected CO<sub>2</sub> and pressure increase in 400 mD case for all gas systems are almost similar to the base case from start of the injection till 1000 years as depicted in Figures 11b and 11c. Table 3 reports the effect of gas type on the cumulative injected CO<sub>2</sub>, total storage of CO<sub>2</sub>, and maximum pressure buildup. However, 400 mD and 800 mD channel permeability values are representative of good quality reservoirs. It seems that the reduction of permeability does not have a remarkable impact on the total injected CO<sub>2</sub> and pressure build up during and after injection. This reduction in permeability doesn't affect the storage potential of CO<sub>2</sub> during the injecting period and more CO immobilizing was observed after injection due to the significant role of residual and dissolution trappings.



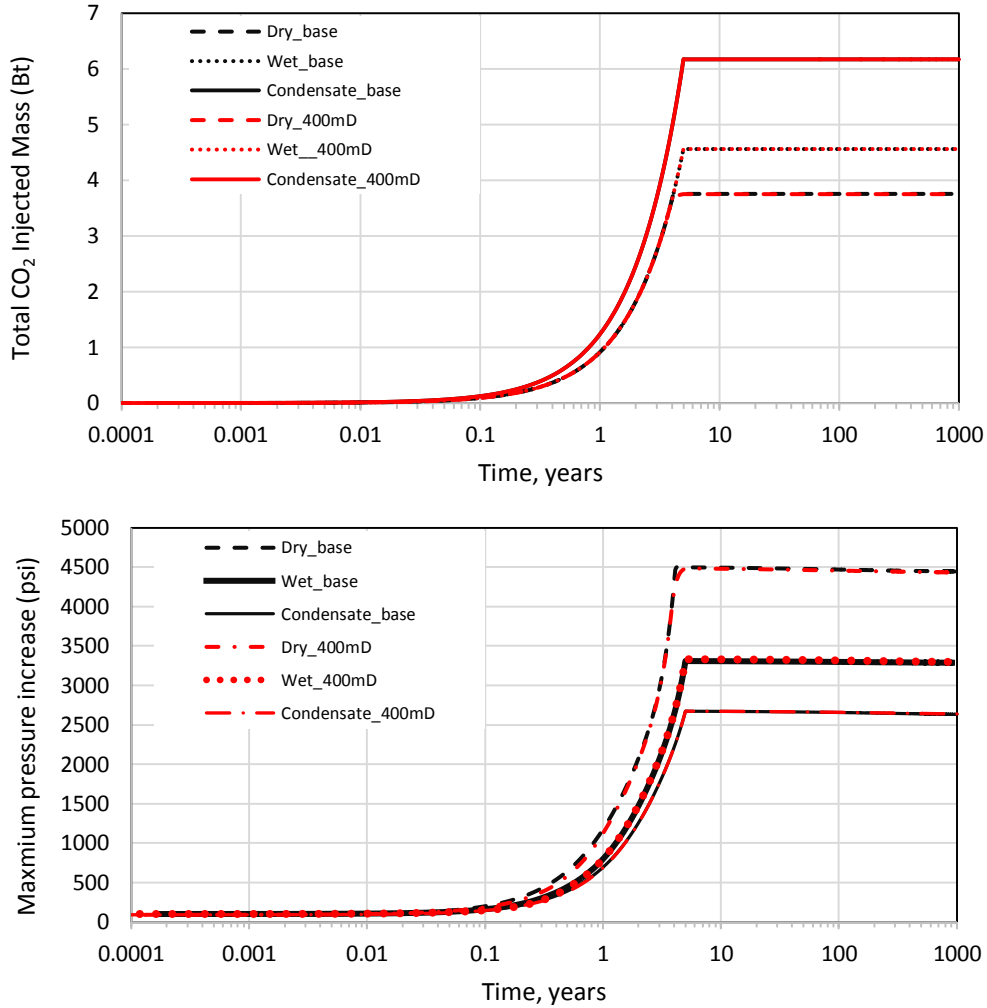


Figure. 11. (a) Comparison of gas mediums for total mass of CO<sub>2</sub> stored at different time for bases case and case\_400mD; (b) The total injected CO<sub>2</sub> mass vs time for bases case and case\_400mD; (c) The maximum pressure buildup vs time for bases case and case\_400mD

Table 4: Comparing the effect of the gas type on cumulative injected CO<sub>2</sub>, total stored CO<sub>2</sub>, and maximum pressure buildup

Case	Gas Type	CONSTRAINTS		Inj. Rate (MScf/D)	Cum. CO <sub>2</sub> Injected (Bt)	CO <sub>2</sub> amount in 1000 years (Bt)			Maximum pressure buildup
		BHP (psia)	Inj. Time (years)			Supercritical free phase	Stored CO <sub>2</sub> as Residual phase	Stored CO <sub>2</sub> as Dissolved in brine	
<b>Base Case</b>	Dry	5000	5	100	3.75	1.14	1.96	0.651	4496
	Wet	5000	5	100	4.55	1.34	2.16	1.05	3307
	Condensate	5000	5	100	6.16	1.84	3.03	1.29	2671
<b>400mD</b>	Dry	5000	5	100	3.75	0.88	2.20	0.67	4481
	Wet	5000	5	100	4.56	1.19	2.30	1.07	3328
	Condensate	5000	5	100	6.17	1.37	3.30	1.50	2670

To assess CO<sub>2</sub> injection into heterogeneous media, two different permeability realizations were considered, as shown in Figure 12, and simulations were run under the same conditions as before. The average channel permeability in these two realizations was 913 mD and 798 mD. The values of permeability in different directions are given in Table 5. As discussed earlier, the heterogeneity factor is related to the gas mixing upon CO<sub>2</sub> injection. Figure 13 shows the results obtained from two different permeability realizations governing the behavior of CO<sub>2</sub> injection.

From Figure13, similar trends for the cumulative amount of CO<sub>2</sub> stored and injected are observed during and after injection in all gas systems which are almost the same trends obtained from the base case. However, little fluctuation in the cumulative amount of CO<sub>2</sub> stored was observed for both permeability realizations (R1 and R2) after the injection period which could be related to the effect of heterogeneity on residual and dissolution trappings. Looking at Table 6, the obtained results for permeability realizations are almost similar to the base case under similar injection conditions. It was then concluded that heterogeneity may not have a significant impact on the storage mechanism of CO<sub>2</sub> in dry, wet and condensate gas systems. However, the permeability variation such as 400mD (see Figure 11) or the one close to a poor-quality storage medium (<10 mD) may offer different storage potentials under certain conditions.

Table 5: Permeability values in different directions in the given realizations

Permeability Realization	K <sub>h</sub>	K <sub>v</sub>	K <sub>z</sub>	K <sub>avg</sub>
	(mD)	(mD)	(mD)	(mD)
<b>R1</b>	1300	1310	130	913
<b>R2</b>	1140	1140	114	798

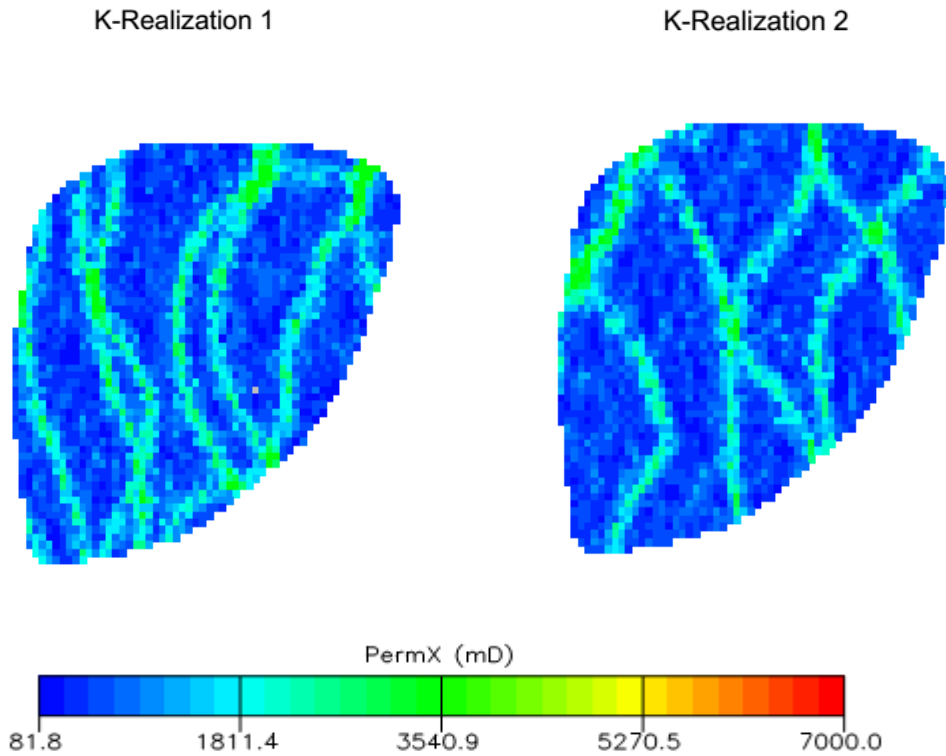


Figure 12. Reservoir models displaying the typical structure of high-permeability meandering channels in a low permeability background for permeability realizations

Table 6. Comparing the effect of gas type on cumulative injected CO<sub>2</sub>, total stored CO<sub>2</sub>, and maximum pressure buildup

Case	Gas Type	CONSTRAINTS		Inj. Rate (MScf/D)	Cum. CO <sub>2</sub> Injected (Bt)	CO <sub>2</sub> amount in 1000 years (Bt)			Maximum pressure buildup
		BHP (psia)	Inj. Time (years)			Supercritical free phase	Stored CO <sub>2</sub> as Residual phase	Stored CO <sub>2</sub> as Dissolved in brine	
Base Case	Dry	8000	5	100	3.75	1.14	1.96	0.651	4496
	Wet	8000	5	100	4.55	1.34	2.16	1.05	3307
	Condensate	8000	5	100	6.16	1.84	3.03	1.29	2671
R1	Dry	8000	5	100	3.78	1.15	1.97	0.66	4497
	Wet	8000	5	100	4.58	1.35	2.17	1.06	3309
	Condensate	8000	5	100	6.20	1.86	3.04	1.30	2673
R2	Dry	8000	5	100	3.72	1.13	1.95	0.64	4495
	Wet	8000	5	100	4.52	1.33	2.15	1.04	3304
	Condensate	8000	5	100	6.21	1.85	3.05	1.31	2670

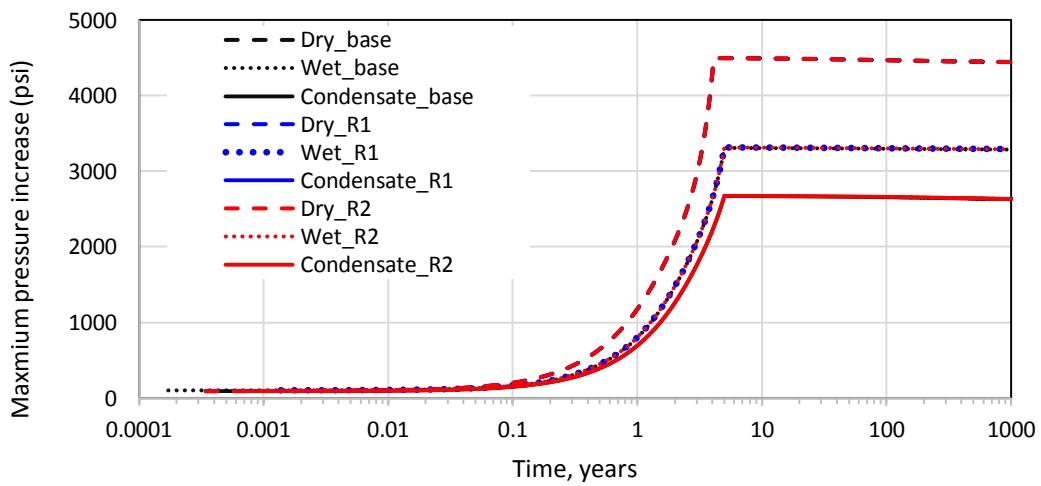
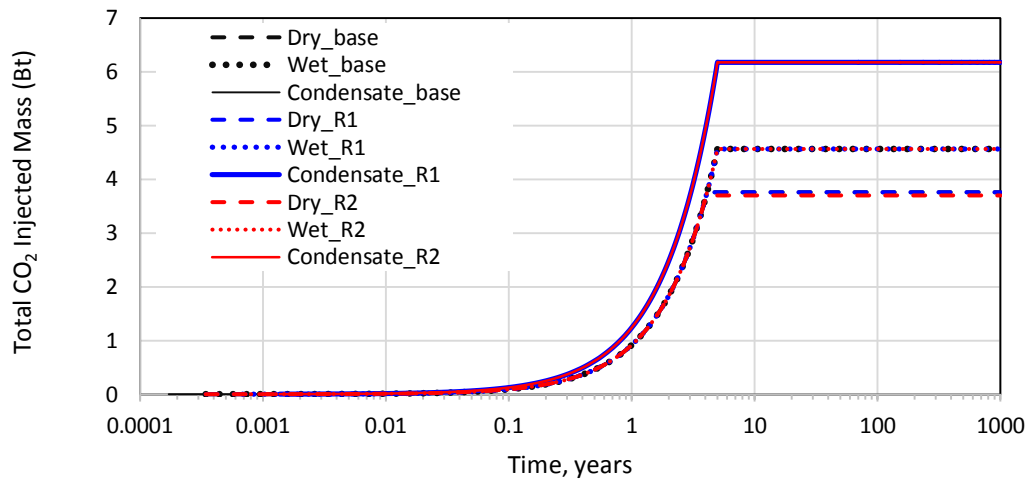
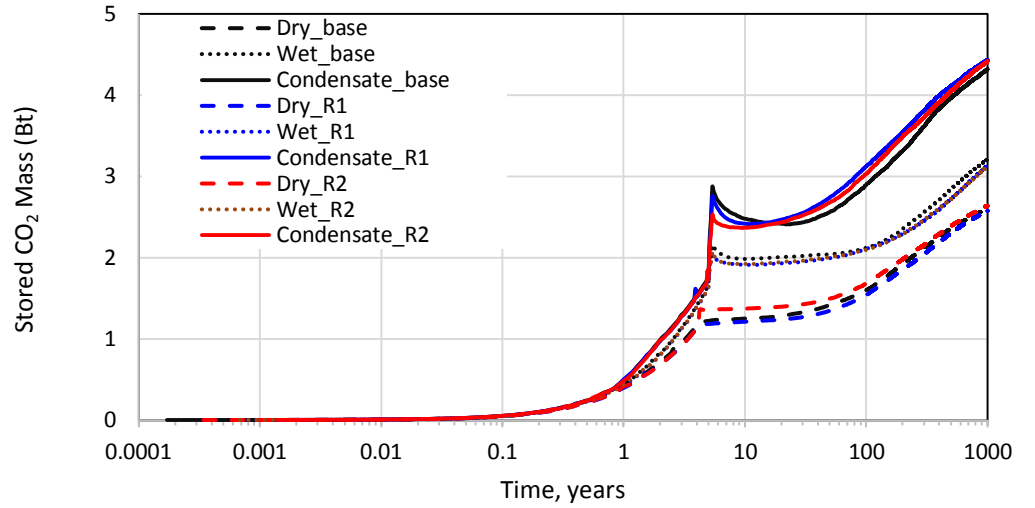


Figure 13: Comparing the amount of CO<sub>2</sub> stored in different gas formations based on two permeability realizations

## 5. Conclusions

A numerical model was built in this study for gas reservoirs to evaluate the long-term storage of CO<sub>2</sub> in gas reservoirs by considering representative compositions of dry, wet and condensate gases. It appears that gas reservoirs have a good potential for CO<sub>2</sub> immobilization in a long-term, but the condensate gas formations would be the best among all three. This could be attributed to the slight remaining gas volume, phase behavior of the condensate gas-CO<sub>2</sub> mixture, good injectivity, and lesser amount of methane mole fractions present in the medium.

A sensitivity analysis was performed to evaluate the variation of the injection rate and heterogeneity on CO<sub>2</sub> storage. It was found that the gas medium storage behavior is sensitive to the injection rate. Selection of an optimum injection rate could help to achieve a high storage potential in gas reservoirs, particularly in condensate gas mediums. Particularly, a high injection rate would also be beneficial for wet gas media to provide a good storage capacity. The results obtained also revealed that reduction in the permeability of the storage site enhances the overall storage capacity by boosting the residual and dissolution trappings after the injection period. Finally, it was concluded that the medium with condensate gas is a more favorable place for storage compared to mediums with dry gas and wet gas.

## Nomenclature

$k$	Permeability
$\mu$	Fluid viscosity
$c_r$	Formation compressibility
$\phi$	Porosity
$F_{pni}^c$	Flow rate component in a phase (p=o, w, g)
$T_{ni}$	Transmissibility between cells n and i
$y_p^c$	Mole fraction of component c in phase p
$k_{rp}$	Relative permeability of phase
$S_p$	Saturation of phase p
$b_p^m$	Molar density of phase p
$\mu_p$	Viscosity of phase p
$dP_{pni}$	Potential difference of phase p between cells n and i, given by
CO <sub>2</sub>	Carbon dioxide
N <sub>2</sub>	Nitrogen
O <sub>2</sub>	Oxygen
SO <sub>2</sub>	Sulfur dioxide
H <sub>2</sub> S	Hydrogen sulfide
P	Pressure
V <sub>M</sub>	Molar volume
R	Gas constant
T	Temperature
A, B	Mixture-specific functions of T and composition with the mixing rules
T <sub>r</sub>	Reduced temperature
C <sub>s</sub>	Salinity
bq <sub>i</sub>	Soreide and Whitson constants
J <sub>i</sub>	Flux of component i per unit area
D <sub>i</sub>	Diffusion coefficient of component i,
$\partial y_i / \partial d$	Molar concentration gradient of component i.
F <sub>ig</sub>	Interblock diffusive flow

$T_D$	Diffusivity, the analogue of transmissibility for diffusive flow
$y_i$	Vapor mole fractions.
$S_g$	Gas saturation
$S_{gi}$	Initial gas saturation
$C$	Land trapping coefficient
$S_{g,max}$	Maximum gas saturation
$S_{gt,max}$	Maximum trapped gas saturation
$K_{rg}^d$	bounding drainage curve
$K_{rg}^{ib}$	bounding imbibition curves
BScf	Billion standard cubic feet
Bt	Billion tones

## Acknowledgment

This work was funded by Curtin Sarawak Research Institute (CSRI) of Curtin University Malaysia under the grant number CSRI-6015. We also acknowledge Schlumberger Malaysia for providing Petrel tool and Eclipse compositional simulator.

## References

1. Bachu S, Gunter W, Perkins E. Aquifer disposal of CO<sub>2</sub>: hydrodynamic and mineral trapping. *Energy Conversion and Management* 35(4):269-79 (1994).
2. McCain Jr WD. Heavy components control reservoir fluid behavior. *Journal of Petroleum Technology* 46(09), 746-750 (1994).
3. Terry RE, Rogers JB. Applied petroleum reservoir engineering. *Pearson hall: Pearson Education*; (2013).
4. Barrufet MA, Bacquet A, Falcone G. Analysis of the storage capacity for CO<sub>2</sub> sequestration of a depleted gas condensate reservoir and a saline aquifer. *Journal of Canadian Petroleum Technology* 49(08):23-31 (2010).
5. Bachu S. Evaluation of CO<sub>2</sub> sequestration capacity in oil and gas reservoirs in the Western Canada Sedimentary Basin. *Alberta Geological Survey, Alberta Energy and Utilities Board March*. (2004).
6. Institute GC. THE GLOBAL STATUS OF CCS | 2016 SUMMARY REPORT. 2016:9-10.
7. Al-Hasami A, Ren S, Tohidi B, editors. CO<sub>2</sub> injection for enhanced gas recovery and geo-storage: reservoir simulation and economics. *SPE Europec/EAGE Annual Conference, Spain, Society of Petroleum Engineers*, (2005):
8. Feather B, Archer R, editors. Enhance natural gas recovery by carbon dioxide injection for storage purposes. *Australia Fluid Mechanics Conference, Auckland, New Zealand*, (2010).
9. Jikich SA, Smith DH, Sams WN, Bromhal GS, editors. Enhanced Gas Recovery (EGR) with carbon dioxide sequestration: A simulation study of effects of injection strategy and operational parameters. *SPE Eastern Regional Meeting, Pennsylvania, 1-9*, (2003).
10. Khan C, Amin R, Madden G. Carbon dioxide injection for enhanced gas recovery and storage (reservoir simulation). *Egyptian Journal of Petroleum* 22(2):225-40 (2013).

11. Khan C, Amin R, Madden G. Effects of CO<sub>2</sub> and acid gas injection on enhanced gas recovery and storage. *Journal of Petroleum Exploration and Production Technology*, 3(1):55-60 (2013).
12. Polak S, Grimstad A-A. Reservoir simulation study of CO<sub>2</sub> storage and CO<sub>2</sub>-EGR in the Atzbach–Schwanenstadt gas field in Austria. *Energy procedia* 1(1):2961-8 (2009).
13. Kühn M, Förster A, Großmann J, Lillie J, Pilz P, Reinicke KM, et al. The Altmark Natural Gas Field is prepared for the Enhanced Gas Recovery Pilot Test with CO<sub>2</sub>. *Energy Procedia*. 37(Supplement C):6777-85 9 (2013).
14. Pamukcu Y, Hurter S, Jammes L, Vu-Hoang D, Pekot L. Characterizing and predicting short term performance for the In Salah Krechba field CCS joint industry project. *Energy Procedia* 4(0):3371-8 (2011).
15. Oldenburg C, Pruess K, Benson SM. Process modeling of CO<sub>2</sub> injection into natural gas reservoirs for carbon sequestration and enhanced gas recovery. *Energy & Fuels* 15(2):293-8 (2001).
16. Azin R, Nasiri A, Entezari J. Underground gas storage in a partially depleted gas reservoir. *Oil & Gas Science and Technology-Revue de l'IFP*.;63(6):691-703 (2008).
17. Narinesingh J, Alexander D. CO<sub>2</sub> enhanced gas recovery and geologic sequestration in condensate reservoir: A simulation study of the effects of injection pressure on condensate recovery from reservoir and CO<sub>2</sub> storage efficiency. *Energy Procedia* 63:3107-15 (2014).
18. Shen C-H, Hsieh B-Z, Tseng C-C, Chen T-L. Case study of CO<sub>2</sub>-IGR and storage in a nearly depleted gas-condensate reservoir in Taiwan. *Energy Procedia* 63:7740-9 (2014).
19. Yuan C, Zhang Z, Liu K. Assessment of the recovery and front contrast of CO<sub>2</sub> EOR and sequestration in a new gas condensate reservoir by compositional simulation and seismic modeling. *Fuel* 142:81-6 (2015).
20. IPCC. IPCC special report on carbon dioxide capture and storage. Prepared by Working Group III of the Intergovernmental Panel on Climate Change. Metz B, Davidson O, De Coninck H, Loos M, Meyer L, editors. Cambridge, United Kingdom and New York, NY, USA (2005).
21. Xiaoling S, Fangui Z, Hejuan L. CO<sub>2</sub>-CH<sub>4</sub> system mixing properties and enhanced natural gas recovery. *International Journal of Digital Content Technology & its Applications*. 6(21):1-5 (2012).
22. Adisoemarta PS, Frailey SM, Lawal AS. Measured Z-Factor of CO<sub>2</sub>-Dry gas/wet gas/gas condensates for CO<sub>2</sub> storage in depleted gas reservoirs. *SPE/DOE Symposium on Improved Oil Recovery, Oklahoma* 1-11; (2004).
23. Sobers L, Frailey S, Lawal A, editors. Geological sequestration of carbon dioxide in depleted gas reservoirs. *SPE/DOE Symposium on Improved Oil Recovery, Oklahoma, Society of Petroleum Engineers* (2004).
24. Loizzo M, Lecampion B, Bérard T, Harichandran A, Jammes L. Reusing O&G-depleted reservoirs for CO<sub>2</sub> storage: Pros and Cons. *SPE Projects, Facilities & Construction*. 5(03):166-72 (2010).

25. Schlumberger. Technical Description 2014;2014.2.
26. Schlumberger. Reference Manual. 2014;2014.2.
27. Soreide I, Whitson CH. Peng-Robinson Predictions for Hydrocarbons, CO<sub>2</sub>, N<sub>2</sub>, and H<sub>2</sub>S with pure water and NaCl brine. *Fluid Phase Equilibria*;77:217-40 (1992).
28. Oldenburg CM. Carbon dioxide as cushion gas for natural gas storage. *Energy & Fuels* 17(1):240-6 (2003).
29. Hoteit H, Firoozabadi A. Numerical modeling of diffusion in fractured media for gas-injection and-recycling schemes. *SPE Journal*. 2009;14(02):323-37.
30. Alavian SA, Whitson CH, editors. Scale dependence of diffusion in naturally fractured reservoirs for CO<sub>2</sub> injection. SPE Improved Oil Recovery Symposium, Oklahoma, USA; (2010).
31. Yanze Y, Clemens T. The role of diffusion for nonequilibrium gas injection into a fractured reservoir. *SPE Reservoir Evaluation & Engineering* 15, 60-71 (2012).
32. Oak MJ. Three-Phase Relative Permeability of Water-Wet Berea. In *SPE/DOE Enhanced Oil Recovery Symposium. Society of Petroleum Engineers* 1-12, (1990)
33. Juanes R, Spiteri E, Orr F, Blunt M. Impact of relative permeability hysteresis on geological CO<sub>2</sub> storage. *Water Resources Research*, 42(12) (2006).
34. Spiteri, E. J, Juanes, R. Impact of relative permeability hysteresis on the numerical simulation of WAG injection, *J. Pet. Sci. Eng.*,50(2)(2006), 115 – 139
35. Bennion DB, Bachu S. Supercritical CO<sub>2</sub> and H<sub>2</sub>S - Brine Drainage and Imbibition Relative Permeability Relationships for Intercrystalline Sandstone and Carbonate Formations. *SPE: Society of Petroleum Engineers* (2006).
36. Land CS. Calculation of imbibition relative permeability for two-and three-phase flow from rock properties. *Society of Petroleum Engineers Journal* 8(02):149-56 (1968).
37. Killough J. Reservoir simulation with history-dependent saturation functions. *Society of Petroleum Engineers Journal* 16(01):37-48 (1976).
38. Jansen JD, Fonseca RM, Kahrobaei S, Siraj M, Van Essen G, Van den Hof P. The Egg Model - data files. TU Delft. Dataset. <http://dx.doi.org/10.4121/uuid:916c86cd-3558-4672-829a-105c62985ab2>. (2013).
39. Kuo C-W, Perrin J-C, Benson SM. Simulation studies of effect of flow rate and small scale heterogeneity on multiphase flow of CO<sub>2</sub> and brine. *Energy Procedia* 4(0):4516-23 (2011).
40. Hingerl FF, Yang F, Pini R, Xiao X, Toney MF, Liu Y, et al. Characterization of heterogeneity in the Heletz sandstone from core to pore scale and quantification of its impact on multiphase flow. *International Journal of Greenhouse Gas Control* 48:69-83 (2016).
41. Han W, Kim K-Y, Esser R, Park E, McPherson B. Sensitivity study of simulation parameters controlling CO<sub>2</sub> trapping mechanisms in saline formations. *Transport in Porous Media*.;90(3):807-29 (2011)
42. Connolly M, Johns RT. Scale-Dependent mixing for adverse mobility ratio flows in heterogeneous porous media. *Transport in Porous Media* 113(1):29-50 (2016).

43. Gershenzon NI, Ritzi RW, Dominic DF, Mehnert E, Okwen RT, Patterson C. CO<sub>2</sub> trapping in reservoirs with fluvial architecture: Sensitivity to heterogeneity in permeability and constitutive relationship parameters for different rock types. *Journal of Petroleum Science and Engineering* (2016).
44. Gershenzon NI, Ritzi Jr RW, Dominic DF, Mehnert E, Okwen RT. Comparison of CO<sub>2</sub> trapping in highly heterogeneous reservoirs with Brooks-Corey and van Genuchten type capillary pressure curves. *Advances in Water Resources*, 96:225-36 (2016).
45. Audigane P, Gaus I, Pruess K, Xu T, editors. A long term 2D vertical modelling study of CO<sub>2</sub> storage at Sleipner (North Sea) using TOUGHREACT. Proceedings, TOUGH Symposium; (2006).
46. Raza A, Rezaee R, Gholami R, Bing CH, Nagarajan R, Hamid MA. A screening criterion for selection of suitable CO<sub>2</sub> storage sites. *Journal of Natural Gas Science and Engineering*.;28:317-27 (2016).
47. Jalil, M., R. Masoudi, N.B. Darman, and M. Othman. Study of the CO<sub>2</sub> injection storage and sequestration in depleted M4 carbonate gas condensate reservoir Malaysia. in Study of the CO<sub>2</sub> injection storage and sequestration in depleted M4 carbonate gas condensate reservoir Malaysia. 2012. Carbon Management Technology Conference.
48. Raza A, Gholami R, Sarmadivaleh M, Tarom N, Rezaee R, Bing CH, et al. Integrity analysis of CO<sub>2</sub> storage sites concerning geochemical-geomechanical interactions in saline aquifers. *Journal of Natural Gas Science and Engineering*, 36PA:224-40 (2016).
49. Ziabakhshganji Z, Kooi H, editors. Equation of State for thermodynamic equilibrium of gas mixtures and brines to allow simulation of the effects of impurities in CO<sub>2</sub> storage. *EGU General Assembly Conference Abstracts* (2012).
50. Chiquet P, Broseta D, Thibeau S. Wettability alteration of caprock minerals by carbon dioxide. *Geofluids*, 7(2):112-22 (2007).
51. Shojai Kaveh N, Barnhoorn A, Wolf KH. Wettability evaluation of silty shale caprocks for CO<sub>2</sub> storage. *International Journal of Greenhouse Gas Control* 49:425-35 (2016).
52. Vilarrasa V, Rutqvist J, Rinaldi AP. Thermal and capillary effects on the caprock mechanical stability at In Salah, Algeria. *Greenhouse Gases: Science and Technology*.;5(4):449-61 (2015).
53. Saeedi A, Rezaee R. Effect of residual natural gas saturation on multiphase flow behaviour during CO<sub>2</sub> geo-sequestration in depleted natural gas reservoirs. *Journal of Petroleum Science and Engineering*, 82–83(0):17-26 (2012).
54. Soroush M, Wessel-Berg D, Kleppe J. Effects of Wetting Behaviour on Residual Trapping in CO<sub>2</sub>-Brine Systems. *SPE: Society of Petroleum Engineers*; (2013).
55. Wildenschild D, Armstrong RT, Herring AL, Young IM, Carey JW. Exploring capillary trapping efficiency as a function of interfacial tension, viscosity, and flow rate. *Energy Procedia*; 4:4945-52 (2011).
56. Shamshiri H, Jafarpour B. Controlled CO<sub>2</sub> injection into heterogeneous geologic formations for improved solubility and residual trapping. *Water Resources Research*, 48(2) (2012).

57. Al Mansoori SK. Impact of carbon dioxide trapping on geological storage: *Imperial College London*; (2009).
58. Kuo C-W, Benson SM. Numerical and analytical study of effects of small scale heterogeneity on CO<sub>2</sub>/brine multiphase flow system in horizontal corefloods. *Advances in Water Resources*, 79(0):1-17 (2015).
59. Raza A, Rezaee R, Gholami R, Rasouli V, Bing CH, Nagarajan R, et al. Injectivity and quantification of capillary trapping for CO<sub>2</sub> storage: A review of influencing parameters. *Journal of Natural Gas Science and Engineering* 26:510-7 (2015).

### **Arshad Raza**

Arshad Raza has B.Sc. and M.Sc. degrees in Petroleum Engineering from UET, Lahore, Pakistan. He had worked in Department of Petroleum & Gas Engineering, UET Lahore, Pakistan since 2010. He obtained his Doctoral Degree from Curtin University, Malaysia in 2017. His research areas are Reservoir Characterization and CO<sub>2</sub> Sequestration.



### **Raof Gholami**

Raof Gholami is a drilling and geomechanical engineer in the Department of Petroleum Engineering at Curtin University, Malaysia. He received his PhD from Shahrood University of Technology, Iran in 2014. He has done several projects related to petroleum geomechanics for various companies. His main research area of interests are wellbore stability and integrity issues, rock characterizations, anisotropy



### **Reza Rezaee**

Professor Reza Rezaee of Curtin's Dept of Petroleum Engineering has a PhD in Reservoir Rharacterization. He has over 25 years' experience in academia. His research has been focused on integrated solutions for reservoir characterization, formation evaluation and petrophysics. Currently, he is working on unconventional gas including gas shale and tight gas sand reservoirs.



### **Chua Han Bing**

Dr. Chua is currently a senior faculty member of the Chemical Engineering Department at Curtin University, Sarawak Malaysia. He obtained his Doctoral Degree from Queen Mary College, London University in 1983. Prior to joining Curtin, Dr. Chua served as a senior academic with a leading tertiary institution in West Malaysia.



### **Ramasamy Nagarajan**

Dr. R. Nagarajan is senior faculty member of the Applied Geology Department at Curtin University Sarawak Malaysia. He completed his PhD at Anna University (India) in 2003. His research area mainly focuses on sediment and environmental geochemistry.

